JOURNAL OF SOLID STATE CHEMISTRY 64, 331–346 (1986)

# Metal–Metal-Bonded Scandium Cluster ($Sc_7Cl_{12}Z$) and Infinite Chain ($Sc_4Cl_6Z$) Phases Stabilized by Interstitial Boron or Nitrogen ($Z$)*,†

SHIOU-JYH HWU AND JOHN D. CORBETT

*Department of Chemistry and Ames Laboratory,§ Iowa State University, Ames, Iowa 50011*

Received December 6, 1985; in revised form March 24, 1986

The title phases have been obtained in high yields from reactions of metal, trichloride, and elemental boron or nitrogen in sealed niobium tubing at 850–950°C. Single crystal structural studies on samples of all four phases obtained by autogenous vapor phase transport reactions are reported. The $Sc_7Cl_{12}Z$ compounds contained discrete $Sc_6Cl_{12}Z$ clusters together with isolated scandium(III) atoms while $Sc_4Cl_{12}Z$ consists of infinite chains of the condensed clusters sharing trans Sc–Sc edges, comparable to those found in $Sc_5Cl_8Z$ and, especially, the closely related $NaMo_4O_6$. The scandium–scandium bond lengths in these reflect both the electron count and the effective interstitial size. Extended-Hückel molecular orbital calculations for both borides demonstrate the prime importance of strong Sc–$Z$ bonding. The chain phases are predicted to be metallic. 

## Introduction

The reduced scandium chlorides have been found to exhibit a remarkable chemistry involving isolated clusters and their condensation products, namely compounds containing discrete clusters, $Sc(Sc_6Cl_{12})$ (*1*), condensed scandium clusters sharing edges in infinite chains, $Sc_5Cl_8$ (*2*), and double chains, $Sc_7Cl_{10}$ (*3*), finally culminating in the double-metal-sheet structure of ScCl (*4*). Equally surprising is that only the monochloride shows a close similarity to compounds formed by the neighboring yttrium, lanthanum, and zirconium. And although interstitial atoms are becoming a popular and significant theme in such compounds, only in the above $Sc(Sc_6Cl_{12})$ example and in $Zr_6Cl_{15}$ was there any crystallographic evidence for an electron density residue in the middle of the cluster, i.e., $Z \sim 4$–5 (*5*).

Subsequent explorations of the possible role and importance of small nonmetals in related zirconium systems have shown that a significant chemistry exists for interstitial hydrogen, carbon, nitrogen, or oxygen in the double-metal-layered ZrX structures (*6–9*). One characteristic of the synthesis of pseudobinary phases in which an adventitious impurity is actually responsible for

* Presented at the Symposium on Synthesis in Solid State Chemistry: Frontier Structures and Novel Results held during the American Chemical Society meeting, Chicago, Ill., September 9–11, 1985.

† The U.S. government's right to retain a nonexclusive, royalty-free license in and to the copyright covering this paper, for governmental purposes, is acknowledged.

§ Operated for the U.S. Department of Energy by Iowa State University under Contract W-7405-Eng-82. This research was supported by the Office of Basic Energy Sciences, Materials Sciences Division.



0022-4596/86 $3.00

TABLE I
SCANDIUM CLUSTER CHLORIDES

| Cl/Sc | Original representation | Structural description | Earlier ref. | Cluster interstitial? | Ref. |
|---|---|---|---|---|---|
| 1.71 | $Sc(Sc_6Cl_{12})$ | Discrete clusters (edge bridged) plus scandium(III) in chloride octahedra | *5* | Yes: B, N | This work |
| 1.60 | $^1_\infty[(ScCl_2^+)(Sc_4Cl_6^-)]$ | Single chains of condensed $Sc_6Cl_{12}$-type clusters plus parallel chains of condensed $ScCl_6$ octahedra | *2* | Yes; C, N | *15* |
| 1.50 | $Sc_2Cl_3$ | Unknown ("mouse fur") | *16* | Probably not | *15* |
| 1.50 | $^1_\infty[Sc_4Cl_6Z]$ | Single chains of condensed $Sc_6Cl_{12}$-type clusters | — | B, N | This work |
| 1.43 | $^1_\infty[(ScCl_2^+)(Sc_6Cl_8^-)]$ | Double chains of condensed $Sc_6Cl_8$ (face-bridged) clusters with parallel chains of condensed $ScCl_6$ octahedra | *3* | Probably not | *15* |
| 1.43 | $^1_\infty[(ScCl_2^+)(Sc_6Cl_8C_2^-)]$ | Double chains of condensed $Sc_6Cl_{12}$-type, carbon-centered clusters with parallel chains of condensed $ScCl_6$ octahedra | — | C | *17* |
| 1.00 | $^2_\infty[Sc_{6/3}Cl_2]$ | Double metal sheets of condensed $Sc_6Cl_8$-type clusters | *4* | H | *15* |
| 1.00 | $^2_\infty[Sc_{6/3}Cl_{6/3}Z]$ | Double metal sheets of condensed, $Z$-centered $Sc_6Cl_{12}$-type clusters | | C, N | *9* |

their stability is the low yield and poor reproducibility of the results, whereas what are properly ternary (or higher) phases are usually obtained in high yields when the correct light atom is added. Thus, zirconium iodide cluster phases have been concluded to be stable only if an interstitial atom is present, not only carbon or boron but also aluminum, silicon, etc. (*10, 11*). This approach to zirconium chloride clusters has yielded a considerable variety of $M^I_x(Zr_6Cl_{12}Z)Cl_y$ phases, $Z$ = Be, B, C, N (*12*), including a nitride that is evidently the same as the previously reported $Zr_6Cl_{15}$ (*1, 5*). Reports of structures involving dicarbon units in gadolinium clusters and cluster chains have also appeared (*13, 14*).

Accordingly, a parallel and subsequent reexamination of the scandium chloride systems has also been undertaken. This has led to the recognition that several, but not all, of the reported scandium chloride phases were probably similarly affected. The present situation is summarized in Table I. In one case, $Sc_7Cl_{10}$, the addition of carbon has been found to produce a distinctive and different structure in $Sc_7Cl_{10}C_2$ (*17*). The present manuscript clarifies the nature of the earlier "$Sc_7Cl_{12}$" and reports the discovery of a new "$Sc_4Cl_6$" phase, each being stable with either boron or nitrogen centered within all metal octahedra. Such a characteristic helps explain the stability of the two electron-poorer cluster phases in Table I with what otherwise appear to be strongly metal–metal bonded structures.

## Experimental Procedures

The scandium metal employed was produced within the Laboratory by the metallothermic reduction of $ScF_3$ by triply distilled Ca. The purity was of the order of >99.9 at.% total with typical impurities in ppm atomic of O-90, N-10, H-320, C-236,

F-185, Fe-39, W-15, and all others, ≤7 each. This was used either in the form of rolled strips about 1.0 × 0.5 × 0.02 cm or as 100-mesh powder produced by the thermal decomposition of $ScH_2$ under high vacuum at 700–750°C. Fusion analysis indicated an H : Sc ratio of about 0.09 : 1 for the latter material. Contamination of such a material by carbon, oxygen, or nitrogen during an unsatisfactory decomposition can be quite effective in producing unexpected ternary phases. It should be noted that oxygen within the metal reacts with $ScCl_3$ to form ScOCl relatively efficiently at these temperatures (*18*).

A 95% amorphous boron (325 mesh, Alpha) as well as a crystalline "5–9's" phase were used (Research Org., Inorg.). The materials obtained with either did not differ significantly as judged from the lattice parameters of the products although the amorphous boron gave more nearly complete reactions. The $NaN_3$ (99%, Aldrich) employed as a nitrogen source was used as received. The $ScCl_3$ synthesis, typical reaction procedures in sealed Nb containers, the mounting of crystals, the Guinier powder photography techniques, lattice constant refinements, crystal diffraction techniques, etc. were carried out as previously described (*3, 5, 17*). The programs utilized for structural calculations, refinements and illustration have been referenced before (*17*). Magnetic susceptibility data between 4 and 340 K were obtained with a SQUID magnetometer on 14 mg of ground single crystals of $Sc_7Cl_{12}B$ sealed in a 3-mm-o.d. silica tube under vacuum.

### *Syntheses*

Typical vacuum and drybox techniques were used whenever the materials were not sealed in niobium reaction containers. The products are moderately air sensitive. Typical reactions involved 150–200 mg $ScCl_3$ and either excess scandium strips or a stoichiometric amount of the powder. Reaction periods as short as 1 week at 860–1000°C will provide powdered products in high yields relative to whichever reactant is limiting. Periods of 4–6 weeks allow better crystal growth via vapor phase transport reactions. Reaction containers within the protective silica jackets were rapidly cooled in air following the reaction periods. Nitrogen from the drybox was used as a source of that element in most cases; the tightly crimped Nb container was inserted into the welder under flowing He and this was evacuated just sufficiently to hold the door in place before rapidly welding the crimped edge.

*$Sc_7Cl_{12}B$.* The polycrystalline material was synthesized in 2 weeks at 860°C from stoichiometric amounts of powdered Sc, $ScCl_3$, and B. The yield was >95%, meaning that no other phase was detectible in the Guinier pattern. Under the same conditions scandium strips gave a visually estimated yield of 80% together with $Sc_2Cl_3$. The latter was the dominant product at 740°C. Single crystals of $Sc_7Cl_{12}B$ were obtained with a 900/940°C gradient and the scandium strips in the hot end. The well-faceted gemlike crystals were found in 25% yield at the cold end of the container while $Sc_4Cl_6B$ in 70% yield was present in the hot end.

*$Sc_7Cl_{12}N$.* The yield of this material at 860–960°C was limited by the amount of $N_2$ that could be retained in the usual Nb container, which is ~10% based on the quantities of Sc and $ScCl_3$ typically used. The single crystals studied were obtained at 950°C in 5 weeks, this giving about 5% each of the phase of interest plus $Sc_5Cl_8N$ and ScOCl. The use of $NaN_3$ instead gave at least an 80% yield of 1T-$Sc_2Cl_2N$ (*9*) at temperatures between 735 and 960°C.

Because of the cavity size in the previously reported $Sc_7Cl_{12}$ and the ubiquity of ScOCl, considerable effort was made to incorporate oxygen into such a phase. However, as before (*17*), these reactions were quite unsuccessful. Attempts to incorpo-

TABLE II

CELL PARAMETERS (Å) AND VOLUMES (Å$^3$) FROM GUINIER POWDER DATA FOR $Sc_7Cl_{12}Z$ AND $Sc_4Cl_6Z$ PHASES[a]

| | *a* | *b* | *c* | *V* | N[b] |
|---|---|---|---|---|---|
| $Sc_7Cl_{12}B$ | 13.014(1) | | 8.899(1) | 1305.4(2) | 27 |
| $Sc_7Cl_{12}N$ | 12.990(2) | | 8.835(1) | 1291.1(4) | 27 |
| $Sc_4Cl_6B$ | 11.741(1) | 12.187(1) | 3.5988(3) | 514.9(1) | 30 |
| $Sc_4Cl_6N(1)$ | 11.634(4) | 12.144(3) | 3.550(3) | 501.5(3) | 24 |
| $Sc_4Cl_6N(2)$ | 11.625(4) | 12.118(3) | 3.5447(7) | 499.3(2) | 15[c] |
| $Sc_4Cl_6N(3)$[d] | 11.625(6) | 12.094(4) | 3.543(2) | 498.0(4) | 18 |

[a] Hexagonal and orthorhombic, respectively.
[b] Number of lines indexed and refined.
[c] Diffractometer data.
[d] Sample prepared from $N_2$.

rate carbon gave instead $Sc_5Cl_8C$ (*15*) or, in more reduced systems, $Sc_7Cl_{10}C_2$ (*17*). Attempts to include Be, F, Si, or Al at 860°C were all unsuccessful. The relative constancy of the Guinier lattice constants for both the boride and the nitride suggest nonstoichiometry is not significant.

*$Sc_4Cl_6B$*. Its crystal preparation was noted above in connection with the synthesis of $Sc_7Cl_{12}B$. One also obtains the $Sc_4Cl_6B$ in 85% yield at 950°C in 2 weeks with stoichiometric amounts of the powders. The visually estimated yield goes to ~100% if three times the necessary amount of boron is used, whereas reactions at the lower temperature of 860°C give only $Sc_7Cl_{12}B$, with mixtures of the two phases at intermediate temperature. The $Sc_7Cl_{12}B$ has also been observed to decompose to this boride at 950°C. Attempts to make $Sc_2Cl_2B$ from the stoichiometric amounts of the reactants at 950°C also gave this phase in ~95% yield based on chlorine. This structure was never encountered when carbon or oxygen had been purposely added to the reaction. The boride could not be intercalated by reaction with KCl or $BaCl_2$ (plus Sc) at 946°C for 1 week, or by Na or K in $NH_3$(l) at room temperature overnight.

*$Sc_4Cl_6N$*. As with the cluster phase above, synthesis of this material was accomplished from elemental nitrogen at 953/940°C for 37 days, the yield evidently being limited only by the quantity of $N_2$ that could be enclosed in the usual reaction container. The use of $NaN_3$ was again unsuitable. All crystals so obtained were seriously defected by twinning (see below).

The structure of this phase was first established from long single crystals obtained in 5–10% yields (based on chloride) from two different $M$Cl:$ScCl_3$:Sc reactions, $M$ = K or Cs, with molar ratios of 4.2:1.6:8.2 (strips) at 960/930°C for 4–9 weeks (plus adventitious nitrogen, presumably). These are crystals 1 and 2, respectively, in subsequent tables. The transported crystals were found in the cooler end of the container, with $Sc_5Cl_8$(N) and $K_2ScCl_5$ or $Cs_3Sc_{2+x}Cl_9$ (*19*) as the other products. They were concluded to be the same nitride phase as synthesized directly (above) by comparison of powder patterns and lattice constants and from the refined occupancies (below).

The lattice constants of the above phases as determined principally by least-squares refinement of Guinier powder data are given in Table II for later reference.

### *Structural Solutions*

Crystal and refinement data for the five studies reported here are contained in Table III.

TABLE III

CRYSTAL AND REFINEMENT DATA FOR SINGLE-CRYSTAL INVESTIGATIONS

| | $Sc_7Cl_{12}B$ | $Sc_7Cl_{12}N$ | $Sc_4Cl_6B$ | $Sc_4Cl_6N(1)$ | $Sc_4Cl_6N(2)$ |
|---|---|---|---|---|---|
| Space group, $Z$ | $R\bar{3}$, 3 | $R\bar{3}$, 3 | *Pbam*, 2 | *Pbam*, 2 | *Pbam*, 2 |
| Crystal dimensions (mm) | 0.46 | 0.26 | 0.40 | 1.50 | 1.50 |
| | 0.30 | 0.20 | 0.02 | 0.02 | 0.03 |
| | 0.25 | 0.14 | 0.02 | 0.04 | 0.06 |
| $2\theta$(max) (deg.) | 55 | 60 | 60 | 50 | 50 |
| Reflections | | | | | |
| Measured | 966[a] | 3071 | 1770 | 2130 | 1899 |
| Observed[b] | 846 | 2060 | 1134 | 1713 | 1426 |
| Independent | 589 | 621 | 580 | 468 | 464 |
| $R$(ave) | 0.016 | 0.061 | 0.030 | 0.065 | 0.065 |
| Absorpt. coeff., $\mu$ ($cm^{-1}$) | 44 | 44 | 40 | 41 | 41 |
| Transm. range | 0.75–1.00 | 0.88–1.00 | 0.89–1.00 | 0.57–1.00 | 0.81–0.99 |
| $R/R_w$ (%)[c] | 3.2/4.0 | 4.2/4.9 | 3.5/4.1 | 8.4/15.1 | 7.7/11.1 |
| Secondary extinction coeff. ($10^{-5}$) | 10.0(1) | 3.2(3) | | | |
| Interstitial occupancy | 1.00(4) | 0.80(2) | 1.05(4) | 1.02(8) | 0.96(6) |
| $B$ ($Å^2$) | 0.1(1) | 0.23[d] | 0.9(2) | 0.5(5) | 1.1(4) |
| $R/R_w$ (%) | 3.0/3.8 | 4.0/4.7 | 3.4/4.0 | 8.4/15.1 | 7.5/11.0 |

[a] Data taken in $\theta$–$2\theta$ scan mode; others were $\omega$-scan.
[b] $F_0 > 3\sigma(F)$, $I_0 > 3\sigma(I)$.
[c] Interstitials at unit occupancy; $R = \Sigma||F_0| - |F_c||/\Sigma|F_0|$; $R_w = [(\Sigma w(|F_0| - |F_c|)^2/\Sigma w|F_0|^2]^{1/2}$.
[d] $B$ fixed at average isotropic value for Sc and Cl.

*$Sc_7Cl_{12}Z$.* These crystals were recognized as having a structure very similar to the reported $Sc_7Cl_{12}$ (*5*) on the basis of lattice constants and symmetry, and this model was found to account well for all lines in the Guinier patterns with respect to both position and intensity. In addition, a Weissenberg photograph of a crystal of $Sc_7Cl_{12}N$ on which data were not taken showed symmetry elements consistent with the space group $R\bar{3}$ and no extra reflections. Refinement started with the earlier heavy atom positions and proceeded uneventfully. For the boride, both the occupancy (1.00(4)) and the isotropic temperature factor of the light atom could be refined, while the smaller nitride crystal gave a lower fraction of observed data, and only the occupancy could be varied (0.80(2)) with a fixed $B$ (Table III). The secondary extinction correction was important for these phases, as has been noted earlier for the refinement of $Zr_6I_{12}C$ (*10*), an analogous structure that lacks only the seventh, isolated metal atom. The isolated Sc(1) atoms were also shown to have effectively unit occupancy. The final difference Fourier maps were flat everywhere to $<1.0$ $e/Å^3$.

*$Sc_4Cl_6Z$.* Crystals of what turned out to be $Sc_4Cl_6N$ first originated from adventitious impurities. The considerable similarity of the first sample to "$\beta$-$Tb_2Br_3$" (*20*) was recognized from a calculated powder pattern based on the positional parameters of the latter. Oscillation photographs about $c^*$ and zero and first level Weissenberg photographs of the $hk$ nets confirmed the reported orthorhombic space group *Pbam* (No. 55). Twinning involving a 90° rotation about a common $c^*$ axis so as to inter-

TABLE IV

POSITIONAL AND THERMAL[a] PARAMETERS FOR $Sc_7Cl_{12}B$ AND $Sc_7Cl_{12}N$

| | $x$ | $y$ | $z$ | $B_{11}$ | $B_{22}$ | $B_{33}$ | $B_{12}$ | $B_{13}$ | $B_{23}$ |
|---|---|---|---|---|---|---|---|---|---|
| $Sc_7Cl_{12}B$ | | | | | | | | | |
| Sc1 | 0.0 | 0.0 | 0.5 | 1.31(3) | 1.31(3) | 4.89(6) | 2.45(3) | 0.0 | 0.0 |
| Sc2 | 0.1630(1) | 0.0439(1) | 0.1502(1) | 0.66(2) | 0.77(2) | 0.90(2) | 0.35(1) | −0.12(1) | −0.05(1) |
| Cl1 | 0.3106(1) | 0.2295(1) | 0.0058(1) | 0.69(2) | 1.10(2) | 1.16(2) | 0.24(1) | −0.16(1) | 0.23(1) |
| Cl2 | 0.1292(1) | 0.1791(1) | 0.3354(1) | 1.11(2) | 1.26(2) | 0.96(2) | 0.67(1) | −0.12(1) | −0.16(1) |
| *B*[b] | 0.0 | 0.0 | 0.0 | 0.10(9) | | | | | |
| $Sc_7Cl_{12}N$ | | | | | | | | | |
| Sc1 | 0.0 | 0.0 | 0.5 | 0.83(5) | 0.83(5) | 6.20(15) | 3.10(8) | 0.0 | 0.0 |
| Sc2 | 0.1616(1) | 0.0438(1) | 0.1492(1) | 0.78(3) | 0.77(3) | 1.12(3) | 0.38(2) | −0.03(2) | −0.04(2) |
| Cl1 | 0.3104(1) | 0.2292(1) | 0.0051(1) | 0.75(3) | 1.17(4) | 1.46(4) | 0.27(3) | −0.14(2) | −0.24(3) |
| Cl2 | 0.1300(1) | 0.1803(1) | 0.3351(1) | 1.20(4) | 1.31(4) | 1.29(4) | 0.71(3) | −0.13(2) | −0.20(2) |
| N[b] | 0.0 | 0.0 | 0.0 | 1.02(12) | | | | | |

[a] $T = \exp[(-\frac{1}{4}(B_{11}h^2a^{*2} + B_{22}k^2b^{*2} + B_{33}l^2c^{*2} + 2B_{12}hka^*b^* + 2B_{13}hla^*c^* + 2B_{23}klb^*c^*)]$: $B_{11} = B_{22}$, $B_{12} = B_{13} = B_{23} = 0$.

[b] Unit occupancy.

change the similar *a* and *b* axes was also indicated by the two sets of festoons observed for both nitride crystals. It was still possible to tune on the major component (ca. 4 : 1) of each crystal and proceed with data collection. The only crystal isolated from nitrogen-added reactions (3, Table II) consisted of about equal proportions of the twin components and showed appreciable overlap of reflections on the Weissenberg. On the other hand, the boron-containing phase showed no twinning even though the difference in the *a* and *b* dimensions is a little less, and so its structural results were better all around. The behavior of the nitride could result from the intrusion of a transition to the tetragonal supergroup *P4/mbm* of the closely analogous Na $Mo_4O_6$ (*21*) below the synthesis temperature.

The refinement started with the heavy atom positions for $\beta$-$Tb_2Br_3$ and proceeded to the end result without event. In all three cases, it proved possible to refine both the occupancy and the thermal parameters of the light atom, the results of these showing good correspondence with the atom indicated (Table III) although the occupancy refinement was not statistically significant for nitride crystal 1. In addition, the lattice constants of the two nitride crystals confirmed that they were the same as purposely prepared, especially for crystal 2 (Table II). The final difference Fourier maps for these three structures were generally flat to less than $<1$ $e/Å^3$ except that the two nitrides showed residuals of 1.2 and 2.5 $e/Å^3$, respectively, at $(\frac{1}{2}, 0, \frac{1}{2})$. This is a conceivable position for intercalated $K^+$ or $Cs^+$ ions that were present during the syntheses. However, the refined occupancies were only 0.08(2) potassium and 0.055(5) cesium ($B \sim 2$), and so these residuals were considered to be artifacts rather than real fractional atoms, presumably originating with crystal imperfections. The 1.50-mm lengths of the crystals may have contributed some errors, but these do not appear to have been serious.

The refined parameters for the five structures studied are reported in Tables IV and V, while the observed and calculated struc-

TABLE V

ATOM POSITIONS AND THE THERMAL PARAMETERS OF $Sc_4Cl_6B$ AND $Sc_4Cl_6N$[a]

| | $x$ | $y$ | $z$ | $B_{11}$[b] | $B_{22}$ | $B_{33}$ | $B_{12}$ |
|---|---|---|---|---|---|---|---|
| $Sc_4Cl_6B$ | | | | | | | |
| Sc1 | 0.3745(1) | 0.3521(1) | 0.5 | 1.32(6) | 1.06(5) | 0.91(5) | −0.14(5) |
| Sc2 | 0.3948(1) | 0.5830(1) | 0.0 | 1.08(5) | 0.86(5) | 0.86(5) | −0.04(4) |
| Cl1 | 0.4794(2) | 0.2407(2) | 0.0 | 1.4(1) | 1.13(5) | 1.20(5) | −0.01(5) |
| Cl2 | 0.2400(2) | 0.4297(2) | 0.0 | 1.23(7) | 1.53(7) | 1.16(6) | −0.06(6) |
| Cl3 | 0.2326(2) | 0.1814(2) | 0.5 | 1.74(8) | 1.65(7) | 1.08(6) | −0.77(6) |
| B | 0.5 | 0.5 | 0.5 | 0.7(1) | | | |
| $Sc_4Cl_6N(1)$ | | | | | | | |
| Sc1 | 0.3770(3) | 0.3522(3) | 0.5 | 1.6(2) | 1.0(1) | 1.8(2) | 0.1(1) |
| Sc2 | 0.3950(3) | 0.5799(3) | 0.0 | 1.2(2) | 1.1(2) | 1.9(2) | −0.2(1) |
| Cl1 | 0.4844(4) | 0.2409(4) | 0.0 | 1.6(2) | 1.3(2) | 1.8(2) | −0.2(1) |
| Cl2 | 0.2401(3) | 0.4270(3) | 0.0 | 1.1(2) | 1.1(2) | 1.7(2) | −0.1(1) |
| Cl3 | 0.2370(4) | 0.1781(4) | 0.5 | 1.9(2) | 1.5(2) | 1.9(2) | −0.2(1) |
| N | 0.5 | 0.5 | 0.5 | 0.5(4) | | | |
| $Sc_4Cl_6N(2)$ | | | | | | | |
| Sc1 | 0.3767(2) | 0.3537(2) | 0.5 | 2.7(1) | 1.3(1) | 1.2(1) | −0.04(8) |
| Sc2 | 0.3970(2) | 0.5803(2) | 0.0 | 2.5(1) | 1.2(1) | 1.2(1) | −0.06(8) |
| Cl1 | 0.4828(3) | 0.2416(3) | 0.0 | 2.9(2) | 1.5(1) | 1.3(1) | 0.1(1) |
| Cl2 | 0.2404(3) | 0.4294(3) | 0.0 | 2.7(1) | 1.7(1) | 1.2(1) | −0.1(1) |
| Cl3 | 0.2340(3) | 0.1790(3) | 0.5 | 3.0(2) | 1.9(1) | 1.2(1) | −0.6(1) |
| N | 0.5 | 0.5 | 0.5 | 1.1(4) | | | |

[a] Unit occupancy of B or N.

[b] $B_{13} = B_{23} = 0$, by symmetry.

ture factors are available as supplementary material.[1]

## Results and Discussion

### *The Clusters $Sc_7Cl_{12}Z$*

The structure of $Sc_7Cl_{12}B$ and $Sc_7Cl_{12}N$ consists of c.c.p. $Sc_6Cl_{12}Z$ clusters with a threefold axis of the clusters normal to the layers and the $Z$ atom in the center of one cluster at the origin. If the layer of clusters including the origin defines the A layer, then the seventh, isolated scandium(1) atom lies along $c$ from an A cluster in chlorine trigonal antiprism between cluster layers B and C, that is, at (0, 0, $\frac{1}{2}$). A description in terms of close-packed chlorine (and $Z$) is also feasible (*22*). The local arrangement along $c$ involving two clusters and the intervening scandium atom is illustrated in Fig. 1 for the nitride while distances and angles in both phases are given in Table VI.

Chlorine atoms shown in the figure have three different functions: six Cl(2) atoms bridge the top and bottom edges of the cluster and also define the antiprismatic cavity for Sc(1). The six Cl(1) atoms bridge the waist edges of the cluster ($Cl^i$) and also pro-

[1] See NAPS document No. 04397 for 11 pages of supplementary material. Order from ASIS/NAPS, Microfiche Publications, P.O. Box 3513, Grand Central Station, New York, NY 10163. Remit in advance $4.00 for microfiche copy or for photocopy, $7.75 up to 20 pages plus $.30 for each additional page. All orders must be prepaid. Institutions and organizations may order by purchase order. However, there is a billing and handling charge for this service of $15. Foreign orders add $4.50 for postage and handling, for the first 20 pages, and $1.00 for additional 10 pages of material. Remit $1.50 for postage of any microfiche orders.

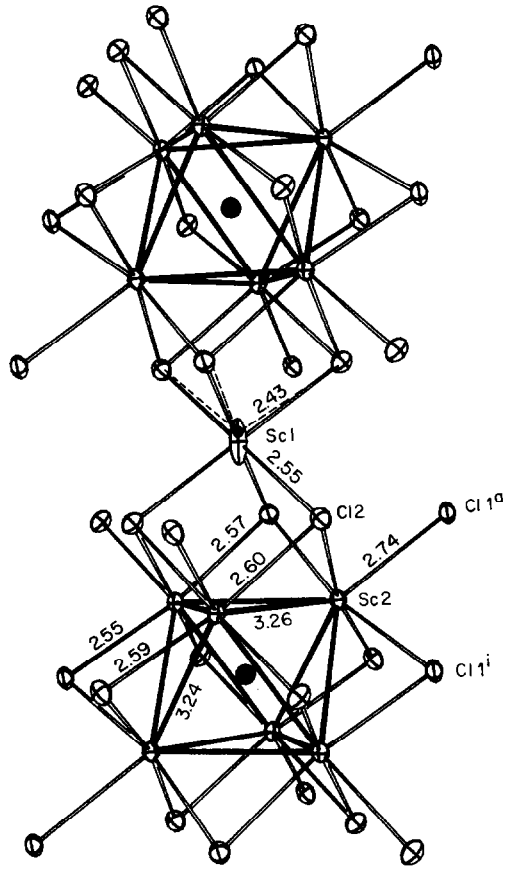


FIG. 1. Two $Sc_6Cl_{12}N$ clusters, the bridging $Cl^a$ atoms from other clusters and the intervening Sc(1) in $Sc_7Cl_{12}N$. (The threefold axis along $c$ is vertical.)

vide the essential bonding to more distant metal vertices in other clusters ($Cl^a$) and vice versa. This yields the functional description $Sc(1)^{3+}[Sc(2)_6(Z)Cl(2)^i_6Cl(1)^{i-a}_{6/2}Cl(1)^{a-i}_{6/2}]^{3-}$ when bonding to the isolated Sc(1) is not included and the bridging chloride is apportioned equally. The different functionality of Cl(1) is probably important in the slight trigonal compression of the scandium antiprism.

The present boride and nitride phases differ mostly in the cluster size. The Sc–$Z$ separation is 0.028 Å less in the nitride, and this results in contractions of 0.037 Å within the end faces of the antiprism and 0.044 Å between these, changes which are also reflected in the increased puckering of the chlorine layers and elongation of the Sc(1) thermal ellipsoid (see below). The chlorine atoms largely follow this cluster contraction so that the principal changes in $d$(Sc–Cl) occur in those to the outer chlorine atoms in other clusters, a change which also parallels increased Sc–$Z$ orbital overlap populations within the nitride cluster (*10*).

The effective interstitial radii in these clusters appear fairly regular and transferable, those in $Sc_7Cl_{12}Z$ being very close to the shorter pair in the rather distorted octahedra in $Sc_4Cl_6Z$ (below). The radii calculated for boron and nitrogen are 1.44 and 1.41 Å, respectively, when a 0.885-Å crystal radius of scandium (III) (*23*) is applied to the separations in $Sc_7Cl_{12}Z$. It is remarkable that the *same* respective values are simi-

TABLE VI

DISTANCES (Å) AND ANGLES (deg) FOR $Sc_7Cl_{12}B$, $Sc_7Cl_{12}N$, AND $Sc_7Cl_{12}$[a]

| | $Sc_7Cl_{12}B$ | $Sc_7Cl_{12}N$ | $Sc_7Cl_{12}$ |
|---|---|---|---|
| Metal cluster | | | |
| Sc1–Sc2 | 3.647(1) | 3.625(1) | 3.627(1) |
| Sc2–Sc2 | 3.293(1) | 2.256(1) | 3.234(1) |
| Sc2–Sc2 | 3.281(1) | 3.237(1) | 3.204(1) |
| Isolated Sc | | | |
| Sc1–Cl2 | 2.547(1) | 2.550(1) | 2.549(1) |
| Metal cluster to chlorine | | | |
| Sc2–Cl1(i)[b] | 2.557(1) | 2.550(1) | 2.540(1) |
| Sc2–Cl1(i) | 2.594(1) | 2.587(1) | 2.576(1) |
| Sc2–Cl1(a) | 2.730(1) | 2.744(1) | 2.755(1) |
| Sc2–Cl2 | 2.577(1) | 2.573(1) | 2.566(1) |
| Sc2–Cl2 | 2.603(1) | 2.595(1) | 2.591(1) |
| Sc2–Cl1–Sc2 | 79.13(2) | 78.12(4) | 77.54(4) |
| Sc2–Cl2–Sc2 | 78.96(3) | 78.10(4) | 77.67(4) |
| Interstitials | | | |
| Sc2–$Z$ | 2.324(1) | 2.296(1) | 2.276(1) |
| Cl1(i)–$Z$ | 3.632(1) | 3.622(1) | 3.610(1) |
| Cl2–$Z$ | 3.639(1) | 3.626(1) | 3.611(1) |

[a] Ref. (*5*).
[b] i = inner, a = outer.

larly deduced from structural data for KCs $Zr_6Cl_{15}B$ and $Zr_6Cl_{15}N$ (*24*).

Comparison of the present results with those found for "$Sc_7Cl_{12}$" formed earlier from adventitious impurities (*5*) (Table VI) shows that the previous cluster was generally slightly smaller than the present nitride, by 0.02 Å in Sc–*Z* and in Sc–Sc within the faces normal to the threefold and 0.03 Å between these. The earlier cell dimensions ($a$ = 12.959(2) Å, $c$ = 8.825(2) Å) are irregularly smaller as well and the volume is also appreciably less. Moreover, the interstitial atom refined to 0.95(3) of an oxygen atom ($R$ = 0.053, $R_w$ = 0.064; 483 reflections, $2\theta < 50°$). These all could be interpreted in terms of an oxygen interstitial in the earlier cluster although attempts to prepare such have been completely unproductive. Of course, crystal growth conditions when trace and possibly mixed interstitials are involved are very different from those obtained during an intentional synthesis.

The elongated thermal ellipsoids of the isolated metal atom have been an unexplained characteristic of a number of compounds with the $Sc_7Cl_{12}Z$ structure. In the present case, the larger value the ratio $B_{33}/B_{11}$ for the isolated Sc(1) atom in the nitride, 7.5 vs 3.7 in the boride, presumably results from the smaller cluster generated by the nitrogen atom and the larger cavity available. In fact, the greater distortion in the nitride allowed this scandium atom to be resolved into a pair, each with 50% occupancy, separated by 0.45 Å along $c$. One of these is marked by the solid dot in the figure. This approximation was originally believed to be unreasonable because of the three short Sc(1)–Cl(2) distances that it generates, 2.43 vs 2.55 Å at the midpoint and 2.58 Å in $ScCl_3$. However, an even greater anisotropy subsequently observed for this atom in $Sc_7Br_{12}C$ and $Sc_7I_{12}C$ has been found to allow both of these to be well refined in the acentric space group $R3$ (*25*). In the iodide this produces not only a well-behaved scandium(1) atom but also a 0.10-Å difference in the edges of the top and bottom triangles of the antiprism, a distortion that is not suggested by the thermal ellipsoids in the present chloride nitride. The oversized cavity generated for the isolated scandium(III) ion between the puckered halogen layers with smaller clusters and larger anions would appear to be at least some of the reason for the behavior. The fact that the average Sc–Sc and Sc–*Z* distances in the bromide and iodide carbides are somewhat *less* than the averages for the chlorides reported here suggests that the greater distortions in the former represent a means of avoiding a greater matrix effect from the larger anions. In the present crystals one cannot distinguish between a microscopic disorder of the isolated metal atom, a macroscopic version of this with twin (polar) domains differing only in the direction of the displacement, or a truly acentric crystal that does not deviate from centricity sufficiently to be refined.

The bonding in these clusters can be readily described with the results of extended-Hückel molecular orbital calculations, as shown in Fig. 2. These have been carried out for both the hypothetical empty cluster $(Sc_6Cl_{12})Cl_6^{9-}$ and $(Sc_6Cl_{12}B)Cl_6^{9-}$ using the observed dimensions of the boride. The parameters used are listed in the supplementary material. Inclusion of the six outer chlorines at appropriate distances is essential for a correct description of cluster bonding since the $\sigma$ bonds from scandium to these transform the same as those to the interstitial atom (*10*). Although the cluster actually has $D_{3d}$ symmetry, deviations from the higher degeneracies in $O_h$ are small, differing in no case by more than 0.1 eV, and so the higher symmetry notation will be used in orbital descriptions.

The orbitals of importance are the metal–metal bonding sets between about −6.5 and −8.5 eV. Those of $a_{1g}$ ($z^2$) and $t_{1u}$ ($xz,yz$)

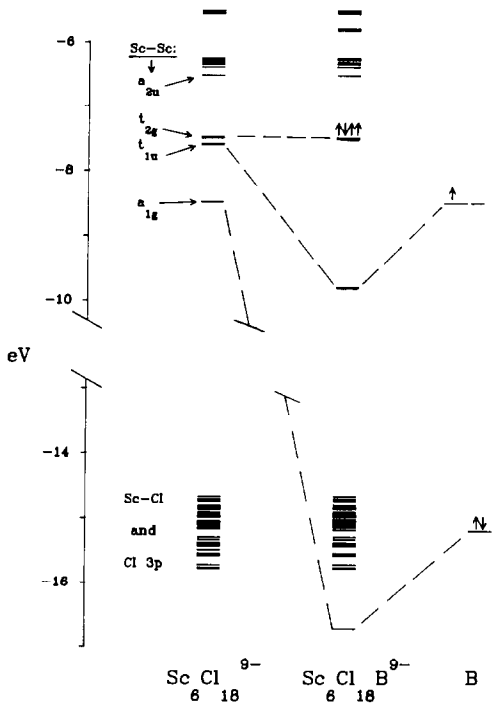


FIG. 2. Molecular orbital diagrams from extended-Hückel calculations: left—empty $(Sc_6Cl_{12})Cl_6^{9-}$ cluster; right—atomic boron; center—$(Sc_6Cl_{12})Cl_6^{9-}$. Orbital labels refer to irreducible representations in $O_h$ symmetry. The HOMO is $t_{2g}^4$.

symmetry naturally interact strongly with the *s* and *p* orbitals of boron to stabilize the cluster through the formation of substantially lower MO's at −16.7 and −9.8 eV, respectively. Although the boron formally donates three electrons to the cluster to produce the $t_{2g}^4$ HOMO (which is also *xz*, *yz* in character), the boron orbitals are filled and lowered in energy substantially and this gives it somewhat of a boride character. The four additional orbitals provided by the interstitial are matched by the appearance of four antibonding sets at high energy. The charge calculated for boron is −1.92, likely a high value by this method, while the occupation of each boron *s* and *p* orbital is 1.45 and 1.16, respectively, indicating something of the covalency and charge transfer to boron when bonded to such an electropositive metal. The insertion of boron reduces the Sc–Sc orbital population of the cluster from 0.19 to 0.07, reflecting the conversion of Sc–Sc to Sc–B bonding. The Sc–Sc separations are typical of those in other arrays (Table I) except for the shorter shared edges of octahedra condensed into chains, centered or not (below, Ref.(*17*)). At the same time, the strong interstitial interaction that is directly opposed to bonding to terminal chlorine appears to give substantial lengthening of the distance to the latter, i.e, 2.73 Å here vs 2.61 Å in the binary $Sc_7Cl_{10}$ (*3*).

The same treatment of the bonding in $Sc_7Cl_{12}N$ reflects the substantial effect that lower $H_{ii}$ values of nitrogen have on the bonding. The resulting $a_{1g}$ and $t_{1u}$ levels now lie at −26.9 and −14.1 eV, respectively, and the $t_{2g}$ HOMO is filled. The inability to substitute oxygen in this structure probably results from the high stability of ScOCl, a further fall of valence energies for the interstitial, and the need to populate the $a_{2u}$ cluster level, an event that occurs only rarely in the more numerous examples of $Zr_6Cl_{12}Z$-type clusters (*12, 24*).

The nominal $t_{2g}^4$ HOMO in $Sc_7Cl_{12}B$ was also examined by magnetic susceptibility measurements; unfortunately, the results are complex. The data shown in Fig. 3 for $\chi$ (mole$^{-1}$) vs *T* at three different fields could be interpreted in terms of some antiferromagnetic ordering below ~180 K, although a phase transition (to *R*3?) cannot be ruled out. The behavior below 50 K could originate from a paramagnetic impurity, e.g., 20 ppm atomic of $Gd^{3+}$, since the expression $\chi = 1.56 \times 10^{-3} + 2.10 \times 10^{-3}/(T - 0.6)$ describes this portion of the data at 2 kG well. Additional experimentation will be necessary to understand the rather complex magnetic features of this compound.

### *Chain Compounds $Sc_4Cl_6Z$*

The phases of $Sc_4Cl_6B$ and $Sc_4Cl_6N$ contain infinite chains of $Sc_6Cl_{12}Z$-type clusters

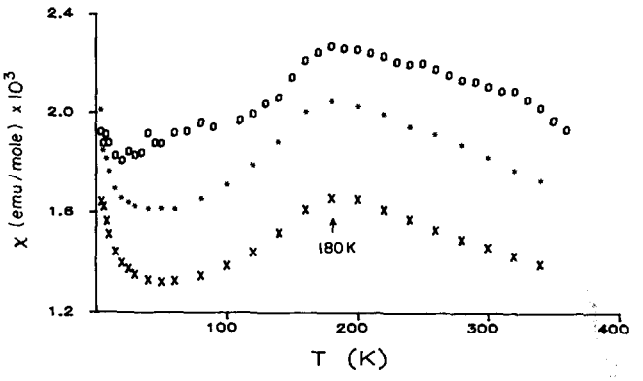


FIG. 3. Molar magnetic susceptibility of $Sc_7Cl_{12}B$ as a function of temperature and field; (○) 1.0 kG, (*) 2.0 kG, (×) 5.0 kG.

sharing trans metal edges and some of the chlorine. A projection of the positions in the boride cell is shown in Fig. 4 along with some selected distances and the atom numbering scheme. Important distances and angles in the boride and in the second nitride crystal are listed in Table VII.

The view in Fig. 4 along the short (3.60 Å) *b* axis has all atoms in layers at $z = 0$ or $\frac{1}{2}$ (dotted spheres). The arrangement will be seen to generate metal octahedra sharing Sc(2)–Sc(2′) edges to form infinite chains. Starting with a $Sc_6Cl_{12}Z$ cluster, two chlorines on the to-be-shared edges of clusters are elimated and the opposite $Sc_2Cl_4$ faces remaining are then shared to give the connectivity $^{1}_{\infty}[Sc(1)_2Sc(2)_{4/2}(Z)Cl(1)^{i}_{4/2}Cl(2)^{i}_{4/2}Cl(3)^{i-a}_{2(2/3)}Cl(3)^{a-i}_{2(1/3)}]$. All chlorine are three-coordinate. The Cl(3) atoms both bridge side edges of the octahedra and bond to the

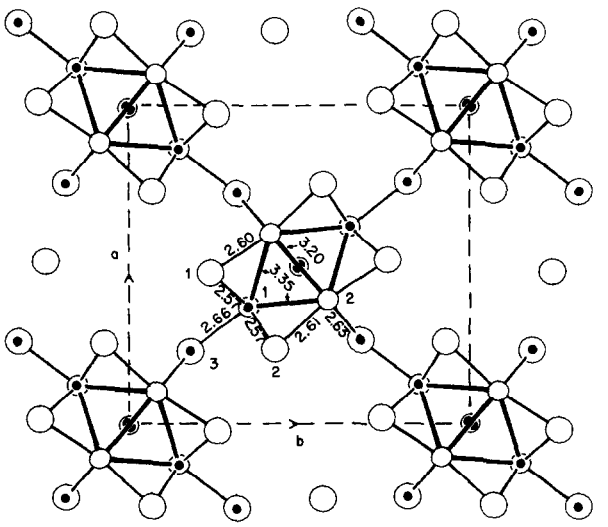


FIG. 4. Projection of $Sc_4Cl_6B$ along [00$\bar{1}$] together with the atom numbering system. Scandium—small spheres connected by heavier lines; boron—centered in scandium octahedra; chlorine—larger spheres. The open spheres are at $z = 0$, dotted spheres, $z = \frac{1}{2}$.

TABLE VII

SELECTED BOND DISTANCES (Å) AND ANGLES (deg) FOR $Sc_4Cl_6B$ AND $Sc_4Cl_6N(2)$

| | $Sc_4Cl_6B$ | $Sc_4Cl_6N(2)$ | | $Sc_4Cl_6B$ | $Sc_4Cl_6N(2)$ |
|---|---|---|---|---|---|
| | Distances | | Angles | | |
| Metal array | | | | | |
| Sc1–Sc2 | 3.351(1) | 3.277(3) | Sc1–Sc2–Sc2a | 61.45(3) | 61.78(8) |
| Sc1–Sc2a[a] | 3.348(1) | 3.271(3) | Sc1–Sc1–Sc2a | 57.01(3) | 56.25(9) |
| Sc2–Sc2a | 3.197(2) | 3.086(5) | Sc1–Sc2–Sc2b | 57.52(1) | 57.26(3) |
| Sc2–Sc2b | 3.5988(3) | 3.545(1) | Sc2–Sc1–Sc2b | 64.96(3) | 65.49(7) |
| Chlorine atoms on metal array | | | Sc1–Sc2a–Sc2e | 57.49(1) | 57.19(4) |
| Sc1–Cl2 | 2.570(1) | 2.551(3) | Sc2a–Sc1–Sc2e | 65.02(3) | 65.62(7) |
| Sc1–Cl2 | 2.572(1) | 2.548(3) | Sc1–Cl1–Sc2a | 80.65(4) | 79.4(1) |
| Sc2a–Cl1 | 2.604(2) | 2.571(4) | Sc1–Cl1–Sc1f | 88.88(5) | 88.0(1) |
| Sc2–Cl2 | 2.606(2) | 2.580(4) | Sc1–Cl2–Sc2 | 80.65(4) | 79.4(1) |
| Sc2–Cl3c(inner) | 2.628(1) | 2.625(3) | Sc1–Cl2–Sc1f | 88.78(5) | 88.1(1) |
| Sc1–Cl3(outer) | 2.664(2) | 2.690(3) | Sc2–Cl3c–Sc2b | 86.41(5) | 85.0(1) |
| Interstitials in metal array | | | Bridging chlorines | | |
| *Z*–Sc1 (×2) | 2.329(1) | 2.279(3) | Sc2–Cl3c–Sc1c | 135.31(3) | 135.75(7) |
| *Z*–Sc2 (×4) | 2.4069(7) | 2.350(1) | Interstitials in metal array | | |
| Nonbonded distances (<3.65 Å) | | | Sc2–*Z*–Sc2a | 83.23(4) | 82.1(1) |
| Cl1–Cl2 | 3.634(2) | 3.622(5) | *Z*–Sc2–Sc2a | 41.62(2) | 41.05(5) |
| Cl1–Cl2d | 3.697(2) | 3.642(5) | | | |
| Cl1–Cl3 | 3.488(2) | 3.475(4) | | | |
| Cl1–Cl3d | 3.602(2) | 3.550(4) | | | |
| Cl2–Cl3 | 3.523(2) | 3.515(4) | | | |
| Cl2–Cl3c | 3.569(2) | 3.518(4) | | | |
| *Z*–Cl1 | 3.644 | 3.604(3) | | | |
| *Z*–Cl2 | 3.644(1) | 3.603(3) | | | |
| *Z*–Cl3 | 3.514(1) | 3.479(4) | | | |

[a] a = $1-x, 1-y, z$; b = $x, y, 1+z$; c = $\frac{1}{2}-x, \frac{1}{2}+y, z$; d = $\frac{1}{2}+x, \frac{1}{2}-y, z$; e = $1-x, 1-y, 1+z$; f = $x, y, z-1$.

exposed Sc(1) vertices in other chains, thus generating a three-dimensional but highly anisotropic structure and fibrous crystals. The chain character and their interconnectivity is further emphasized by the perspective view along [½, 0, *z*] shown in Fig. 5 where actual thermal ellipsoids have been employed. Judging from Weissenberg photographs and the thermal ellipsoids, the crystals studied were relatively well ordered for a structure in which there is predominant one-dimensional bonding.

It should be noted that the idealized octahedra from which these chains are constructed have been characteristically distorted in the process. The shared edge, 3.20 Å in $Sc_4Cl_6B$, is the shortest Sc–Sc distance, from these to the scandium(1) apices is next, 3.35 Å, while the repeat distance along the chain is 3.60 Å (the *b* axis). The corresponding distances in the nitride are 0.05–0.08 Å less following a 0.04-Å decrease in the average Sc–*Z* separation. The chain period is reasonable and even necessary if there are to be chlorine atoms on the chain with the same repeat; in other words, Cl–Cl closed-shell repulsions are likely responsible for the relative elongation of

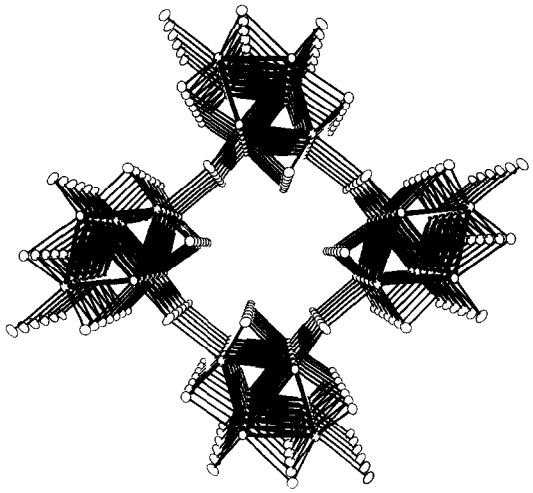


FIG. 5. A perspective view of four chains in $Sc_4Cl_6B$ centered about [1/2, 0, $z$] and drawn with 50% probability thermal ellipsoids. The scandium atoms are interconnected by heavier lines.

these octahedra. The general impression from this structure and others (Table I, Refs. (*26, 27*)) is that the metal chains are well sheathed by chloride. The symmetry of the "octahedra" in the present case is $C_{2h}$ but these are within three standard deviations of $D_{2h}$.

Chains of exactly the same construction have been found in $Sc_5Cl_8$ (*2*) (actually $Sc_5Cl_8(C, N)$ (*15*)). This structure can be derived from that in Fig. 4 by replacing a pair of opposed chains by chains of $Sc^{III}Cl_6^{3-}$ octahedra also sharing trans edges so as to retain the same interchain connectivity, namely, $^1_\infty[ScCl_{4(1/3)}Cl^+_{2(1/3)}]$. Likewise, the structure of $NaMo_4O_6$ (*21*) is very closely related to that of $Sc_4Cl_6Z$, the principal difference being that the molybdenum compound is tetragonal with planar oxygen atom interconnections between the chains and sodium ions in the cavities between groups of four chains. Removal of the sodium can be imagined to cause the structure to "sag" to orthorhombic symmetry with 167° angles at bridging chlorine (Fig. 4). The result still appears to be relatively open. The model compound "$\beta$-$Tb_2Br_3$" was suspected to be impurity-stabilized from the beginning (*20*); the large cavities therein (leading to the appelation *Heissluft*) are about the right size to contain silicon. The three structures have been compared (*28*).

The scandium(III-chlorine) chains in $Sc_5Cl_8Z$ formally donate additional electrons to the $Sc_4Cl_6Z$ chains (*2*), and the distances in $Sc_5Cl_8C$ are accordingly somewhat shorter than the average in $Sc_4Cl_6B$ and $Sc_4Cl_6N$, by 0.10 Å in the shared Sc–Sc edge and 0.08 Å in the scandium waist–apex separations. The Sc–$Cl^i$ distances about the chain are also about 0.02 Å less in the carbide. The absence of the compound $Sc_4Cl_6C$ appears to be a consequence of the high stability of the neighboring $Sc_7Cl_{10}C_2$ with a similar Cl : Sc ratio. The somewhat larger dimensions observed for $Sc_4Cl_6N$, crystal 1, may have resulted from the presence of mixed adventitious impurities, especially a small amount of carbon. However, a few attempts to prepare phases with mixed interstitials directly have not been successful, giving instead only known ternary compounds. Interestingly, the structure of $Y_4Cl_6$, which has not been found to date for scandium, involves face-capping of similar metal chain octahedra by chlorine and *no* interstitial atoms (*27*), presumably would otherwise provide unreasonably short Cl–$Z$ separations (*17*).

Although cluster condensation is an attractive way to relate a structure such as Sc ($Sc_6Cl_{12}B$) to that of $Sc_4Cl_6B$ geometrically, the process should not be taken too literally. The actually reaction is stoichiometrically complex, viz., either

$$Sc_7Cl_{12}B \xrightarrow{\Delta B} \tfrac{3}{2}Sc_4Cl_6B + ScCl_3$$

or

$$Sc_7Cl_{12}B \rightarrow Sc_4Cl_6B + Sc_2Cl_3 + ScCl_3.$$

Something like the second can be accomplished directly at 950°C, but electronically the process is more complex. Based on a theoretical study of cluster condensation of $Zr_6Cl_{12}C$-type clusters to the double-metal-sheet structure $Zr_2Cl_2C$ (*29*), we expect an analogous scrambling of Sc–Sc bonding states will take place as the scandium cluster is stripped of chlorine and then condensed, although the Sc–B bonding states will be well preserved through this process.

Analogous to the bonding deduced for single interstitial atoms in other isolated and condensed systems (*10–12, 14, 29*), we expect the valence orbitals of boron or nitrogen in $Sc_4Cl_6Z$ will be well utilized in forming Sc–Z (and Sc–Sc) bonding states or, in other words, the nonmetal bands will be filled. This means that only one or three electrons per formula unit will be left for a scandium conduction band in $Sc_4Cl_6B$ or $Sc_4Cl_6N$, respectively (namely, 12 − 6 − 3 in the latter), or 1.5 or 4.5 electrons when this is based on six metal atoms. These counts are, in fact, *less* than those in $Sc(Sc_6Cl_{12}Z)$, which contain 4 (B) or 6 (N) electrons per cluster when the isolated atom is plausibly taken to be scandium(III). Thus clusters rather than chains form in the presence of a higher chlorine and a lower relative interstitial level even though there are more electrons left for metal–metal bonding in the cluster. The simple cluster compound $Sc_6Cl_{12}Z$ with the $Zr_6I_{12}C$ structure (*10*) and only 1–3 extra electrons would clearly be a poor third. The shorter metal–metal distances observed in the clusters, 3.25 Å in $Sc_7Cl_{12}B$ vs 3.33 Å in condensed $Sc_4Cl_6Z$, are consistent with the foregoing conclusions. We suspect that Sc–Sc distances in such cases are, in fact, determined to a considerable degree by the effective size of the interstitial and the Sc–$Z$ interactions in the particular polyhedron involved, analogous to the prime importance of $M$–$Z$ separations in rock salt structures (matrix effects).

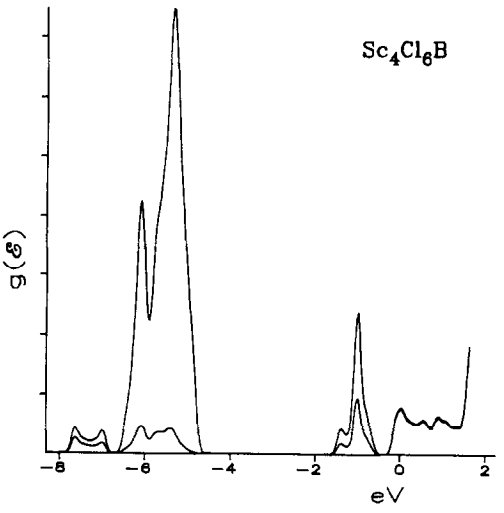


FIG. 6. The total density of states vs the binding energy calculated for $Sc_4Cl_6B$ by extended-Hückel methods ($E_F = 0$). The principal atom and orbital contributions to each of the four bands (and the atom contribution given by the insert) are, from left to right: boron 2*s* and scandium 3d (B), chlorine 2*p* and scandium 3*d* (Sc), boron 2*p* and scandium 3*d* (B), and scandium 3*d*.

Finally, experimental determination of even the qualitative conduction features of the $Sc_4Cl_6Z$ phases would appear to be particularly difficult because of both their fibrous habit and, especially, their moisture sensitivity. On the other hand, extended-Hückel calculations have been found to give a good account of the UPS valence spectra of the infinite double-metal-layered phases ZrCl, $Zr_2Cl_2C$, and $Sc_2Cl_2C$ and their conduction properties (*29*) as well as some understanding of the bonding in such phases and in $NaMo_4O_6$ (*30*). Therefore, a calculation on a single $Sc_4Cl_6B$ chain together with the necessary bridging chlorine at the vertices of the metal octahedra has been carried out at 26 *k* points in reciprocal space using standard parameters (supplementary material) and the same programs.

The density of states results obtained for the valence region of $Sc_4Cl_6B$ are shown in Fig. 6. The top curve gives the total density

of states while inset curves show one important contribution to each feature. The large and familiar (*31*) peak around −5.5 eV contains chlorine 2*p* and Sc–Cl bonding states, the inset showing the scandium 3*d* contribution with chlorine 2*p* making up substantially all of the difference. Peaks at about −7.5 and −1.0 eV are principally boron and scandium derived, the insets showing boron 2*s* and 2*p* components, respectively, and reflect the important covalent bonding of the interstitial to metal. There are somewhat more metal than boron states in the boron p band, and significant Sc–Sc bonding therein as well judging from overlap populations. Finally, the conduction band from −0.3 to +2.0 eV is substantially all scandium in character, again a characteristic result. Boron–scandium overlap populations are relatively evenly distributed between apical and equatorial (shared edge) scandium atoms, as might be expected from the structure, while the equitorial scandium pair with their smaller separation contribute a larger overlap population to the bottom parts of the two nominal boron valence bands. The two classes of Sc–Sc bonding in the conduction band are about equal in overlap population up to $E_F$, where above the equitorial–equitorial part falls to zero at +0.6 eV and the apical–equitorial, at +1.0 eV. The distribution of a.o.'s in these bands is consistent with the results for $NaMo_4O_6$ (*30*) given the added boron and the elongation of the octahedra along the chain.

There seems to be little doubt that $Sc_4Cl_6B$ is metallic in character. Furthermore, substitution of beryllium would seem unlikely as this would (in a rigid band) lower the Fermi level into the 2*p* band, an unfavorable prospect. Moreover, the greater size of beryllium would require substantial expansion of the cluster and loss of equitorial–apex metal–metal bonding since a compensating shortening of the chain does not seem feasible based on the size of the chlorine. On the other hand, the states above $E_F$ are bonding, and the observed nitride formation ($E_F$ = +0.4 eV in a rigid model) would also allow the formation of somewhat shorter Sc–Sc bonds.

This somewhat open structure contains cavities between the chains that appear suitable for intercalcated atoms, i.e., ~3.45 Å in radius at ($\frac{1}{2}$, $\frac{1}{2}$, 0), Fig. 4, analogous to $NaMo_4O_6$. However, attempts to intercalate the boride with potassium or barium at 950°C or with sodium or potassium in liquid ammonia at room temperature have been unproductive judging from the lattice constants, the total range observed for all experiments being only +0.04% in *a*, +0.08% in *b*, and −0.04% in *c* relative to the parent phase. The problem with predicting such chemistry by theory is a long standing one and stems from one's inability to make good judgments without a knowledge of the stability of *all* alternate phases, some of which may be unknown. The answer to the present negative results is probably no more profound than the possibility that KCl and $BaCl_2$ have greater stability.

## Acknowledgments

The authors are indebted to Professor R. A. Jacobson for the X-ray diffraction and computing facilities, to Professor R. N. Shelton for the magnetic susceptibility measurements, and to Dr. S. Wijeyesekera and R. P. Ziebarth for assistance in the extended-Hückel calculations.

## References

1. J. D. Corbett, R. L. Daake, K. R. Poeppelmeier, and D. H. Guthrie, *J. Amer. Chem. Soc.* **100,** 652 (1978).
2. K. R. Poeppelmeier and J. D. Corbett, *J. Amer. Chem. Soc.* **100,** 5039 (1978).
3. K. R. Poeppelmeier and J. D. Corbett, *Inorg. Chem.* **16,** 1107 (1977).
4. K. R. Poeppelmeier and J. D. Corbett, *Inorg. Chem.* **16,** 694 (1977).
5. J. D. Corbett, K. R. Poepplemeier, and R. L. Daake, *Z. Anorg. Allg. Chem.* **491,** 51 (1982).
6. A. W. Struss and J. D. Corbett, *Inorg. Chem.* **16,** 360 (1977).

7. L. M. SEAVERSON AND J. D. CORBETT, *Inorg. Chem.* **22,** 3202 (1983).
8. J. E. FORD, J. D. CORBETT, AND S.-J. HWU, *Inorg. Chem.* **22,** 2789 (1983).
9. S.-J. HWU, R. P. ZIEBARTH, S. V. WINBUSH, J. E. FORD, AND J. D. CORBETT, *Inorg. Chem.* **25,** 283 (1986).
10. J. D. SMITH AND J. D. CORBETT, *J. Amer. Chem. Soc.* **107,** 5704 (1985).
11. J. D. SMITH AND J. D. CORBETT, *J. Amer. Chem. Soc.* **108,** 1927 (1986).
12. R. P. ZIEBARTH AND J. D. CORBETT, *J. Amer. Chem. Soc.* **107,** 4571 (1985).
13. E. WARKENTINE, R. MASSE, AND A. SIMON, *Z. Anorg. Allg. Chem.* **491,** 323 (1982).
14. A. SIMON AND E. WARKENTIN, *Z. Anorg. Allg. Chem.* **497,** 79 (1983).
15. S.-J. HWU AND J. D. CORBETT, unpublished research.
16. B. C. MCCOLLUM, M. J. CAMP, AND J. D. CORBETT, *Inorg. Chem.* **12,** 778 (1973).
17. S.-J. HWU, J. D. CORBETT, AND K. R. POEPPLEMEIER, *J. Solid State Chem.* **57,** 43 (1985).
18. J. D. CORBETT, J. D. SMITH, AND E. GARCIA, *J. Less-Common Met.* **115,** 343 (1986).
19. K. R. POEPPELMEIER, J. D. CORBETT, T. P. MCMULLEN, D. R. TORGESON, AND R. G. BARNES, *Inorg. Chem.* **19,** 129 (1980).
20. HJ. MATTAUSCH, R. EGER, AND A. SIMON, unpublished research (1979).
21. C. C. TORARDI AND R. E. MCCARLEY, *J. Amer. Chem. Soc.* **101,** 3963 (1979).
22. H. IMOTO, J. D. CORBETT, AND A. CISAR, *Inorg. Chem.* **20,** 145 (1981).
23. R. D. SHANNON, *Acta. Crystallogr. Sect. A* **32,** 751 (1976).
24. R. P. ZIEBARTH AND J. D. CORBETT, unpublished research.
25. D. S. DUDIS, J. D. CORBETT, AND S.-J. HWU, submitted for publication.
26. J. D. CORBETT, *Adv. Chem. Ser.* **186,** 329 (1980).
27. HJ. MATTAUSCH, J. B. HENDRICKS, R. EGER, J. D. CORBETT, AND A. SIMON, *Inorg. Chem.* **19,** 2128 (1980).
28. J. D. CORBETT, *Acc. Chem. Res.* **14,** 239 (1981).
29. R. P. ZIEBARTH, S.-J. HWU, AND J. D. CORBETT, *J. Amer. Chem. Soc.* **108,** 2594 (1986).
30. T. HUGHBANKS AND R. HOFFMANN, *J. Amer. Chem. Soc.* **105,** 3528 (1983).
31. J. D. CORBETT AND J. W. ANDEREGG, *Inorg. Chem.* **19,** 3822 (1980).